Table 2. Positions of flux minima for electron energies greater than 1.1 MeV compared to positions of satellite L shells.

Satellite		Position of minimum		
			Offset dipole L	
Name	Minimum L shell	Centered dipole L	Inbound	Outbound
Miranda	5.0	5.6	5.2	5.2
Ariel	7.4	7.9	7.6	7.6
Umbriel	10.3	10.6	10.8	10.2

(*10*). When the rotation period was also allowed to vary, the best-fit period obtained was 17.4 hours, and with the 17.4-hour period, the best-fit orientation of the dipole was the same to within 0.1° in both tilt angle and direction. Because we have only three feature pairs to use in the model fit, the assignment of formal uncertainties is difficult. However, as illustrated in Fig. 5, the best-fit values of both the tilt angle and the tilt direction are well determined (probably to better than 0.5° and 1°, respectively), and the rotation period is determined to better than 0.5 hour.

The tilt angle, tilt direction longitude, and rotation rate were determined independent of the results obtained by Ness (*2*) and Warwick (*11*) and their colleagues from their analysis of Voyager 2 data. The parameters of the resulting models are in good agreement, even though the magnetometer model also includes an offset from the center of Uranus. Our analysis provides an independent measurement of the large tilt angle and direction of the lowest order (dipole) term as well as of the rotation period of the planetary interior.

The large angle between the magnetic dipole and rotation axes causes each satellite to sweep out a wide range in L during each half-rotation of Uranus (Fig. 1). Absorption of charged particles, however, is most effective near the minimum L shell of each satellite. There are two reasons for this effect: (i) each satellite spends most of its time in the band of L shells near its minimum, and (ii) when a satellite is not near its minimum L shell, it is at higher latitudes and cannot absorb particles that mirror at smaller magnetic latitudes. Thus the minima in the particle absorption signatures are expected to occur near the minimum L shell of each satellite.

As illustrated in Table 2, however, the L shells where absorption signature minima were observed were generally outside these expected locations. With the centered dipole model, these deviations were 0.3 to 0.6 in L, increasing toward smaller values of L; with the offset dipole model (*2*), the deviations were significantly smaller (0.2 in L), except at Umbriel. These results suggest that high-order moments of the field are important to the field geometry.

As shown in Table 2, the offset dipole model does not accurately describe the electron drift shell at Umbriel, perhaps because Umbriel is at a distance from Uranus where external contributions to the field are important. The inbound-outbound asymmetry in the position of Umbriel's signature is in the same direction as the drift shell asymmetry expected from dayside compression of the magnetosphere. Further analysis of these results will lead to better values of the internal and external components of the magnetic field at Uranus.

REFERENCES AND NOTES

1. For a description of the CRS system on Voyagers 1 and 2, see E. C. Stone *et al.*, *Space Sci. Rev.* **21**, 355 (1977).
2. N. F. Ness *et al.*, *Science* **233**, 85 (1986).
3. We define L as $R/\cos^2(\lambda)$, where R is the radial distance from the center of the offset magnetic dipole in Uranus radii ($1\ R_U = 25{,}600$ km) and λ is the magnetic latitude. The rotational pole currently illuminated by the sun is the southern (negative latitude) pole, as defined by the International Astronomical Union.
4. Counting rates were obtained from the following detectors of the CRS instrument: D1 ($\gtrsim$1.1-MeV electrons), $G \sim 11$ cm^2 sr, 100% duty cycle; C4 (high gain, $\gtrsim$3.1-MeV electrons), $G \sim 20$ cm^2 sr, 3% duty cycle; C4 (low gain, $\gtrsim$7.6-MeV electrons), $G \sim 13$ cm^2 sr, 3% duty cycle; L1 (no gain change, $\gtrsim$0.43-MeV protons and pile-up of $\gtrsim$20-keV electrons), $G \sim 4.5$ cm^2 sr, 100% duty cycle (Fig. 3, curve 1); B2, C4, C3, and C2 (coincidence, low gain, 63- and 160-MeV protons and $\gtrsim$70-MeV helium), $G \sim 11$ cm^2 sr, 50% duty cycle (Fig. 3, curve 3) [see (*1*) for more information].
5. J. A. Van Allen *et al.*, *J. Geophys. Res.* **85**, 5709 (1980).
6. R. E. Vogt *et al.*, *Science* **215**, 577 (1982).
7. A. W. Schardt and F. B. McDonald, *J. Geophys. Res.* **88**, 8923 (1983).
8. J. R. Thomas and W. R. Doherty, *JPL Tech. Mem. 33-543* (1972), p. 315.
9. M. Schulz and L. J. Lanzerotti, *Particle Diffusion in the Radiation Belts*, (Springer-Verlag, New York, 1974).
10. The longitude system used here is that recommended by the Voyager Project Office, in which the longitude of Voyager 2 at 1800 spacecraft event time on 24 January 1986 was +121° (where positive longitudes are measured clockwise as viewed from above the rotation pole currently illuminated by the sun).
11. J. W. Warwick *et al.*, *Science* **233**, 102 (1986).

12. We thank R. E. Vogt for his contributions during his tenure as principal investigator for the CRS system on Voyager 2; we are also indebted to the late A. W. Schardt, whose contributions to the analysis of the CRS data at Jupiter and Saturn were an important factor in our understanding of the Uranian magnetosphere. We thank the Voyager project members and the enthusiastic staff of our laboratories at Caltech and Goddard Space Flight Center for their excellent support; special thanks go to P. Schuster, T. Garrard, R. Burrell, L. Thomas, and O. Divers. Supported by NASA under contracts NAS7-918 and NGR 05-002-160. D.L.C. was supported in part by the Aerospace Corporation's sponsored research program.

31 March 1986; accepted 5 May 1986

The Magnetosphere of Uranus: Hot Plasma and Radiation Environment

S. M. Krimigis, T. P. Armstrong, W. I. Axford, A. F. Cheng, G. Gloeckler, D. C. Hamilton, E. P. Keath, L. J. Lanzerotti, B. H. Mauk

The low-energy charged-particle (LECP) instrument on Voyager 2 measured low-energy electrons and ions near and within the magnetosphere of Uranus. Initial analysis of the LECP measurements has revealed the following. (i) The magnetospheric particle population consists principally of protons and electrons having energies to at least 4 and 1.2 megaelectron volts, respectively, with electron intensities substantially exceeding proton intensities at a given energy. (ii) The intensity profile for both particle species shows evidence that the particles were swept by planetary satellites out to at least the orbit of Titania. (iii) The ion and electron spectra may be described by a Maxwellian core at low energies (less than about 200 kiloelectron volts) and a power law at high energies (greater than about 590 kiloelectron volts; exponent γ, 3 to 10) except inside the orbit of Miranda, where power-law spectra (γ approximately 1.1 and 3.1 for electrons and protons, respectively) are observed. (iv) At ion energies between 0.6 and 1 megaelectron volt per nucleon, the composition is dominated by protons with a minor fraction (about 10^{-3}) of molecular hydrogen; the lower limit for the ratio of hydrogen to helium is greater than 10^4. (v) The proton population is sufficiently intense that fluences greater than 10^{16} per square centimeter can accumulate in 10^4 to 10^5 years; such fluences are sufficient to polymerize carbon monoxide and methane ice surfaces. The overall morphology of Uranus' magnetosphere resembles that of Jupiter, as evidenced by the fact that the spacecraft crossed the plasma sheet through the dawn magnetosheath twice per planetary rotation period (17.3 hours). Uranus' magnetosphere differs from that of Jupiter and of Saturn in that the plasma β is at most 0.1 rather than 1. Therefore, little distortion of the field is expected from particle loading at distances less than about 15 Uranus radii.

Studies of magnetospheres in the solar system are a central objective of planetary exploration and have greatly enhanced understanding of astrophysical plasmas (*1*). Voyager 2 carried the low-energy charged-particle (LECP) experiment, whose scientific objectives are to determine the intensity, energy spectra, composition, angular distributions, and spatial and temporal characteristics of ions ($E \gtrsim 28$ keV) and electrons ($E \gtrsim 22$ keV). The large tilt of Uranus' magnetic dipole axis (~60°) (*2*) with respect to the rotation axis, the rapid planetary rotation (17.3 hours) (*3*), and the five major satellites within the magnetosphere present an intriguing magnetospheric configuration.

The LECP instrument has two sensor systems: the low-energy particle telescope and the low-energy magnetospheric particle analyzer, both of which have a large number of solid-state detectors arranged in telescope configurations that can be used in various coincidence-anticoincidence arrangements (*4*). Individual angular distributions during the instrument's passage through Uranus' magnetosphere were obtained every 12.8 minutes by rotating the detector apertures through eight 45° sectors in two complete scans which lasted a total of 96 seconds. At all other times throughout the encounter, the instrument was held stationary in sector 7 (*4*), viewing the general direction of expected magnetosphere corotation or toward the dawn magnetosphere. Continuous stepping of the instrument was resumed approximately 18 hours after closest approach, with one full 360° scan made every 384 seconds.

Overview. Figure 1 shows the count rate of approximately 28-keV ions measured for 10 days surrounding closest approach of the spacecraft to the planet. A general increase in particle activity began on day 21, with an obvious particle enhancement starting at a distance of about 140 Uranus radii (R_U, or 25,600 km) early on day 22 and lasting approximately 12 hours. The activity continued to increase on day 23 with several enhancements upstream; on day 24 there was a large increase (by a factor of about 100) just before the bow shock encounter. Although an interplanetary component was generally present from the solar direction, specific enhancements showed predominant flow from the direction of the planet. The large increases before the bow shock encounter suggest that the magnetosphere may well have extended to beyond 30 R_U at earlier times (*5*).

The ion intensity increased to 10^3 times the interplanetary intensities after the spacecraft crossed the magnetopause (Fig. 1). Significant structure was seen in the flux inside the magnetosphere. The count rate dropped to nearly interplanetary levels before the end of day 24; three encounters with the plasma sheet were observed on day 25, coincident with the reported neutral sheet crossings (*2*). Even after Voyager crossed the nominal magnetopause early on day 26, increases in ion intensities were observed on days 26 and 27. These increases suggest that additional encounters of the plasma sheet may have occurred before the outbound bow shock crossings.

Figure 2 shows an overview of most LECP channels for about 30 hours surrounding closest approach. The parameter L, the equatorial crossing radius of a dipole field line in units of R_U, was calculated from the field model of Ness and colleagues (*2*). Upstream activity for low-energy ions (shown explicitly in Fig. 1) is evident, as is the corresponding activity in the intensity of energetic electrons. A small, 1-hour enhancement in the low-energy electrons and ions follows the bow shock (BS) crossing. The magnetopause (first M) entry is more distinctive in the case of the electrons than for the ions. A shoulder appears at the minimum L-shell crossing of Titania (T) for both the energetic protons ($\gtrsim 100$ keV) and intermediate-energy electrons ($\gtrsim 200$ keV). Distinct absorption features appear at the minimum L-shell crossings of all the major satellites.

The sharp drop-off at most energies for both ions and electrons occurred in the vicinity of the outbound L-shell crossing at Titania. Some low-energy ions were present outside this L shell, but their intensities approached background at the nominal location of Oberon's L shell. Distinct increases in the spectra of the low-energy ions at about 0300 and 0600 spacecraft event time on 25 January and of the electrons at about 0630 suggest encounters of Voyager with the magnetospheric plasma sheet. A crossing at about 1200 spacecraft event time on the same day (Fig. 1) shows some evidence of plasma outflow.

Satellite signatures. Using the offset tilted dipole magnetic field model of Ness and colleagues (*2*), we computed L values throughout the encounter and plotted the data against this parameter in Fig. 3, which shows the inbound and outbound trajectories for selected ion and electron channels. Intensities of electrons (top curve) during the outbound trajectory were mostly higher inside Ariel's orbit than during the inbound trajectory because of the spacecraft's proximity to the magnetic equator (inset). Ap-

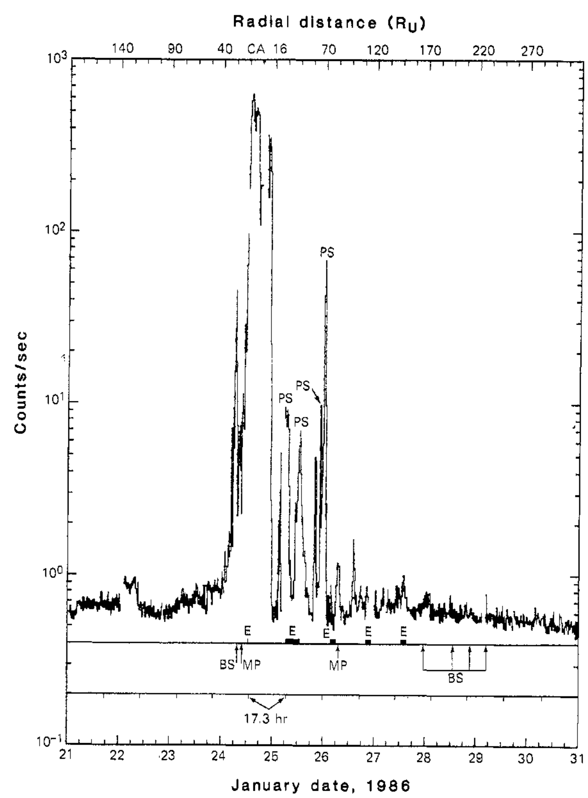

Fig. 1. Intensity of low-energy ions (28 to 43 keV) as a function of spacecraft event time during the Uranus encounter. Ion enhancements began early on day 21, before bow shock (BS) and magnetopause (MP) crossings. After the sharp decrease in count rate near 2300 on day 24, there are four encounters with the plasma sheet (PS). Times of nominal magnetic dipole equator crossings are shown by heavy bars marked (E). Tick marks indicating the planetary rotation period (17.3 hours) are noted on the line below the curve; the phase was chosen to coincide with the first magnetotail neutral sheet crossing. Several bow shock crossings occurred from day 27 through day 29 (*2*). Ion intensities did not return to interplanetary background levels until the middle of day 30.

S. M. Krimigis, A. F. Cheng, E. P. Keath, B. H. Mauk, Applied Physics Laboratory, Johns Hopkins University, Laurel, MD 20707.
T. P. Armstrong, Department of Physics and Astronomy, University of Kansas, Lawrence, KS 66044.
W. I. Axford, Max-Planck-Institüt für Aeronomie, 3411 Lindau, Federal Republic of Germany.
G. Gloeckler and D. C. Hamilton, Department of Astronomy, University of Maryland, College Park, MD 20742.
L. J. Lanzerotti, AT&T Bell Laboratories, Murray Hill, NJ 07974.

parent satellite signatures near the orbits of Miranda, Ariel, and Umbriel are evident during both segments of the trajectory. The absorption signatures, however, do not appear to coincide with the nominal L-shell values of the satellites inbound and outbound: for example, the minimum at the orbit of Ariel outbound occurs exactly at the nominal value ($L \sim 7.4$), whereas the inbound minimum occurs at $L \sim 7.2$. The minimum for the Umbriel signature occurs at $L \sim 10.8$ inbound and at $L \sim 10.2$ outbound, bracketing the nominal value ($L \sim 10.4$). These discrepancies may well be related to uncertainties in the field model.

The inbound-outbound asymmetry is substantially greater for ions inside the orbit of Ariel in a similar energy range, as shown in the second set of curves in Fig. 3. Here satellite "microsignatures" (absorption due to a recent satellite encounter) may also be present at $L \sim 7.2$ and possibly at $L \sim 8.6$. On the outbound trajectory, there are intensity features close to the orbits of both Miranda and Ariel but no clear signature at the orbit of Umbriel. The Ariel features, however, do not seem to coincide with the signatures in the electron intensity profile.

The third and fourth curves in Fig. 3 show the L profile of 61- to 112-keV electrons and 43- to 80-keV ions, respectively, with apparent features close to the orbits of

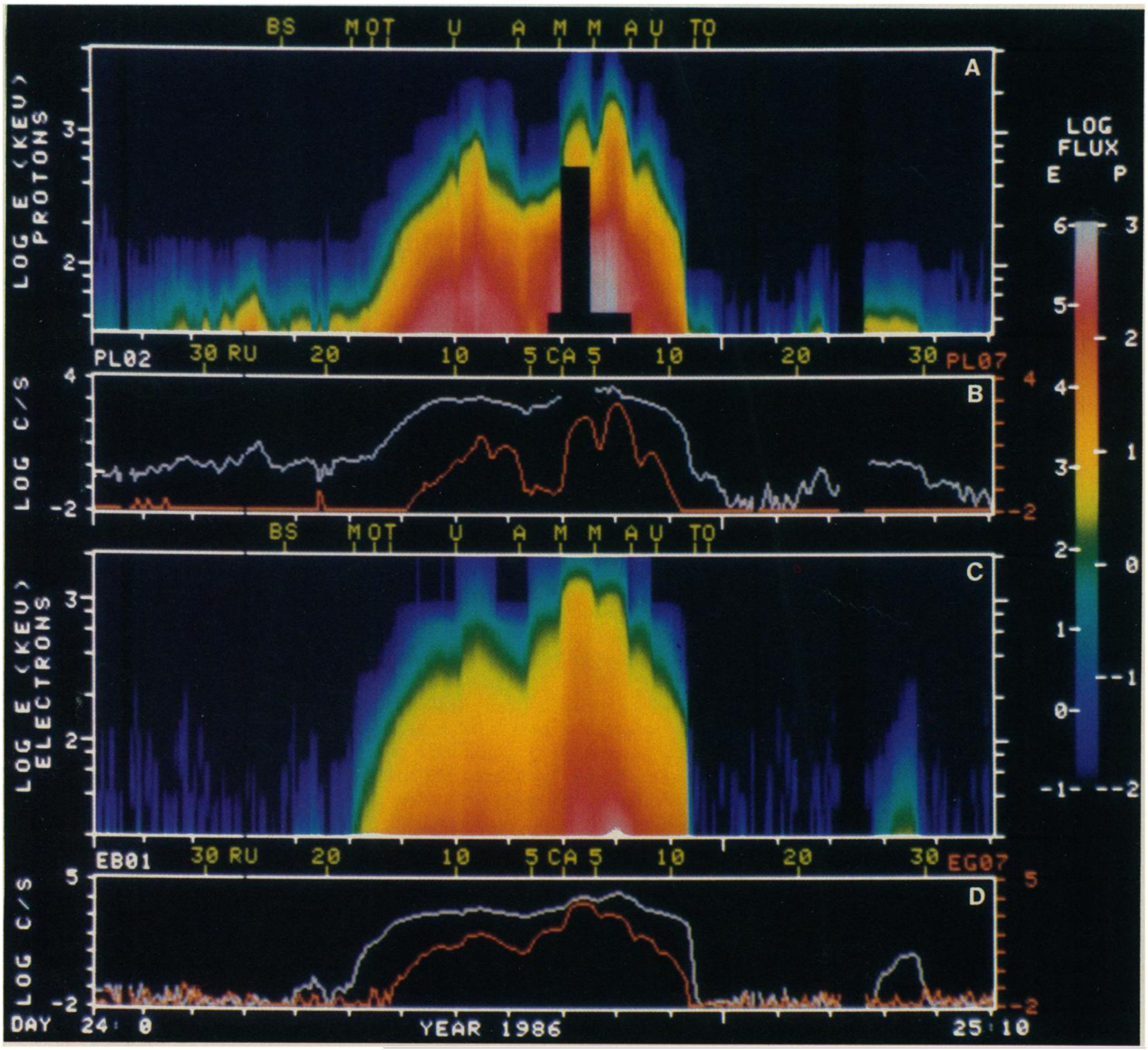

Fig. 2. Spectrograms of energetic ions (A) and electrons (C) from 0000 spacecraft event time on day 24 through 1000 on day 25. The bow shock (BS), magnetopause (first M), and minimum satellite L-shell (O, T, U, A, M) crossing times are shown on the tops of these panels. The electron fluxes are generally much greater than the proton fluxes at a given energy throughout the encounter (note the different color-scaling levels for protons and electrons to the right of the figure). The low-energy proton data surrounding closest approach have been deleted because of substantial contamination of some channels by high-energy electrons. (B) Intensity-time traces for protons of about 40 keV (white curve) and 1 MeV (orange curve). The radial distance of the spacecraft from the center of the planet is indicated at the top of this panel. (D) Intensity-time traces for electrons of about 22 keV (white curve) and 480 keV (orange curve). The first encounter of the magnetotail plasma sheet peaked at approximately 0600 spacecraft event time on day 25.

Miranda and Ariel inbound but no such features anywhere on the outbound trajectory. The intensity outbound decreases sharply at $L \sim 16.5$, just inside the orbit of Titania; there is a large inbound-outbound asymmetry outside $L \sim 16$.

Spectra. Figure 4 shows electron (A) and ion (B) spectra for selected periods. The lower of the two electron spectra in Fig. 4A,

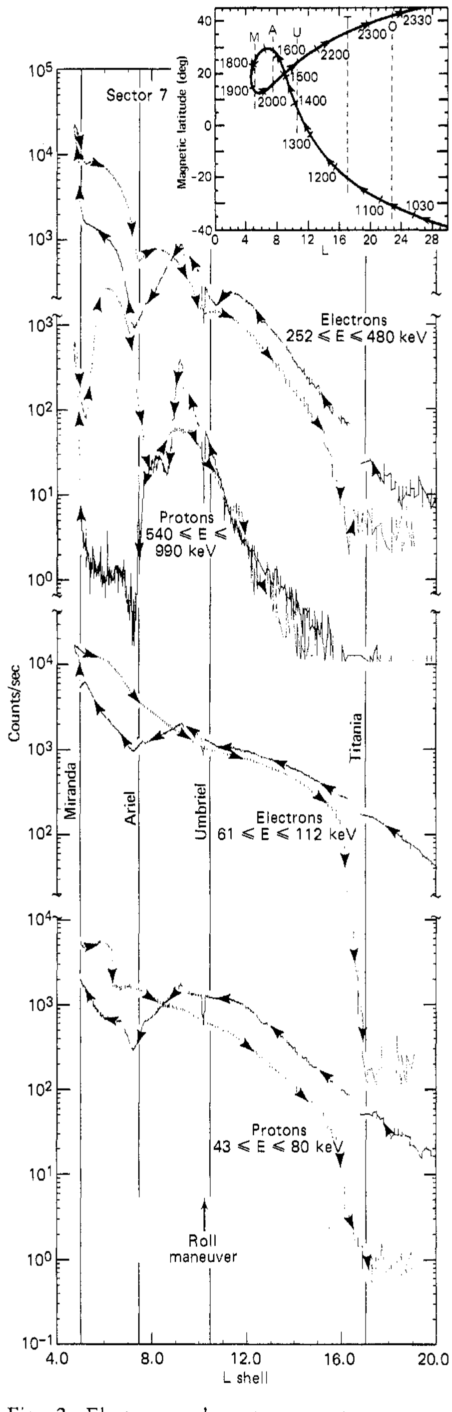

Fig. 3. Electron and proton count rates as a function of L for selected energy channels. (Inset) Voyager 2's trajectory in magnetic latitude as a function of L computed from the model of Ness and co-workers (*2*). Note the dayside-nightside asymmetries in particle intensities at large L values (16 to 20) for low-energy electrons and ions.

sampled between the L shells of Ariel and Umbriel, shows a power-law tail with $\gamma \sim 2.7$. The subtle roll-off at lower energies suggests a Maxwellian core [$kT \sim 15$ keV (k, Boltzmann's constant; T, temperature in kelvins)]. The other electron spectrum, sampled inside the L shell of Miranda, is hard and can be characterized by a simple power law with $\gamma \sim 1.1$. Because such a spectrum cannot be generated readily by simple inward diffusion, a cosmic ray albedo neutron decay source is an obvious candidate, provided that a sharp cutoff exists somewhat beyond the LECP energy coverage (~1.2 MeV). The full ion spectrum shows a Maxwellian core ($kT \sim 35$ keV) much more clearly than the corresponding electron spectrum. At higher energies the ion spectra all show nonthermal tails. The spectrum becomes substantially harder inside the orbit of Miranda.

Composition. The LECP instrument separated the ion species at energies greater than about 0.6 MeV per nucleon during the encounter (*6*). Only one species other than protons, molecular hydrogen (presumably ionized), was identified above that energy. The 1-hour ion mass histogram in Fig. 5 (characteristic of the full encounter) shows the H_2 events appearing as a shoulder on the large proton peak. H_3 and ^4He ions, both of which were observed at Jupiter and Saturn, are absent; no more than one or two counts from these species was measured during the entire encounter. The H_2:H abundance is approximately $1:10^3$ during the period shown and is even lower in other parts of the magnetosphere. Upper limits of 1 in 10^4 protons can be placed on the H_3 and ^4He ions. These relative abundances are much lower than those observed at Jupiter and Saturn (*7*).

Discussion. It is of interest to compare the energetic particle populations in the magnetosphere of Uranus, Jupiter, and Saturn as studied by the LECP instrument. The apparent periodicity in plasma sheet encounters, modulated by Uranus' rotation period, is reminiscent of Jupiter's magnetosphere, although only a few cycles are evident at Uranus because of the rapidity of the instrument's passage through the much smaller magnetosphere. Such a periodicity was also detected in electron spectral indices at Saturn (*8*). Furthermore, Uranian plasma sheet encounters were apparently observed in energetic ion channels when the outbound spacecraft was presumably in the magnetosheath and even as it crossed in and out of the bow shock from 27 through 29 January. In addition, modulation of the proton intensities upstream of the planet, before encounter of the bow shock, seems to be generally in phase with the planetary rotation period. The directionality of the ions and the presence of energetic electrons in these upstream particle increases (Fig. 2) indicates that the observed upstream ions originated from within the planetary magnetosphere, as is the case at Jupiter (*9*) and probably Saturn and Earth (*10, 11*).

A second important characteristic of the Uranian energetic particle intensities is the effect of their having been swept by planetary satellites embedded within the magnetosphere. The satellite absorption signatures in the radiation belts are complicated by the tilt of the dipole moment with respect to the rotation axis. A particular satellite sweeps particles from its minimum (equatorial) L

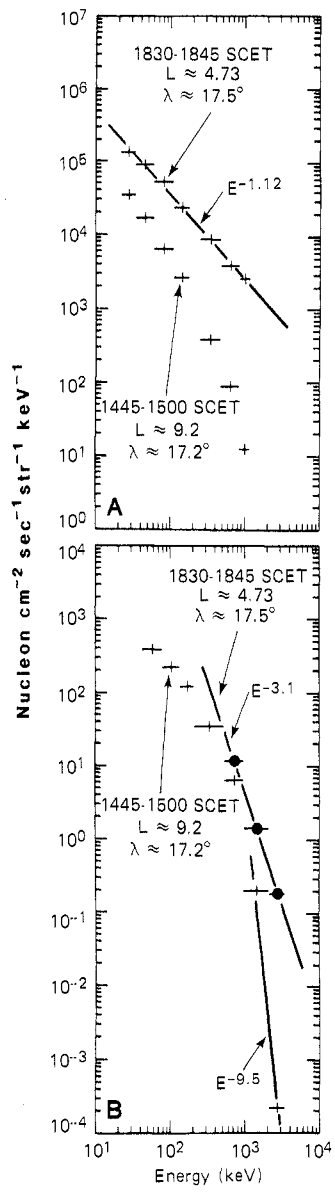

Fig. 4. Electron (A) and proton (B) spectra at selected locations within the Uranian magnetosphere. The electron and ion spectra sampled inside the orbit of Miranda were fit with power-law forms (fits represented by solid lines). Abbreviation: SCET, spacecraft event time.

value to values extending beyond the magnetosphere. This effect must be included in identifying a specific absorption feature with a particular planetary satellite. Figure 3, for example, shows that the absorption of energetic electrons at the orbit of Ariel seems to be substantially inward of the apparent absorption for energetic protons in a similar energy range. This apparent discrepancy is not readily explainable and may be related to the location of the satellite with respect to the spacecraft.

Absorption signatures are nearly absent in the low-energy electron flux and, to a lesser extent, the low-energy ion flux. The electron observations can be attributed to resonant sweeping, whereby electrons of the appropriate energy have an azimuthal drift period nearly equal to the satellite orbital period; such electrons are not effectively swept by the satellite. The resonant electron energies here are roughly 50 to 100 keV, similar to the energies of LECP electron channels in which satellite absorption is not evident. Obviously this effect does not account for the lack of such signatures in the low-energy ion channels. Losses due to charge exchange may, however, be important for the low-energy ions.

The energy spectra of protons measured in the magnetosphere of Uranus have shapes similar to those observed at both Jupiter and Saturn; the spectra are often characterized by a power law at the higher energies but roll off at lower energies ($\lesssim$200 keV), which suggests Maxwellian cores. The temperatures inferred from the Maxwellian fits are similar to those found at Jupiter and Saturn [$kT \sim$ 10 to 50 keV (*5, 12*)]. At high energies, the spectra are extremely steep, with power-law exponents in the range of 3 to 10. The maximum ion intensities at Uranus are much lower than those measured at Jupiter or Earth and are comparable to those at Saturn. Initial estimates show that the plasma β (ratio of particle pressure to magnetic field pressure) for the LECP-measured ions is at most approximately 0.1 at $L \lesssim 15$, which is a factor of about 10 less than the ratio observed at Jupiter and Saturn (*5, 12*). Since the pressures of the low-energy plasma are similarly small (*13*), it is likely that the magnetic field of Uranus is relatively undistorted by particle stresses, in contrast with the case at Jupiter and Saturn.

The population of energetic ions is essentially completely dominated by protons, with a very small fraction of H_2 ions. If this measured composition persists at lower energies as well, then the magnetosphere plasma population will be dominated by an internal source, with a relatively unimportant solar wind source. It is likely that the extended hydrogen atmosphere identified

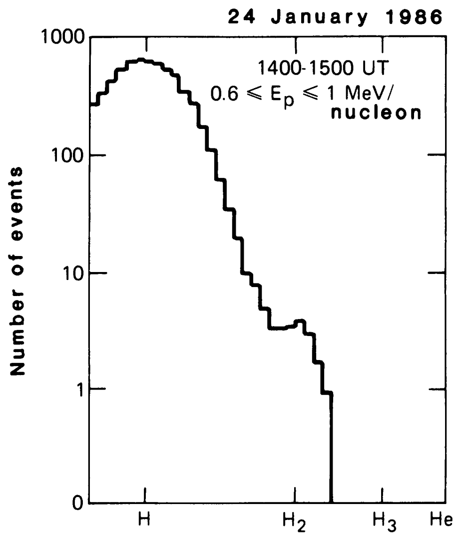

Fig. 5. Logarithmic histogram of pulse height–analyzed events in the low-energy particle telescope detector system. The shoulder to the right of the proton distribution indicates H_2 ions in the magnetosphere of Uranus.

by the Voyager 2 UVS instrument (*14*) is also evidence for an atmospheric source of the magnetospheric plasma.

Energetic protons in the magnetosphere continuously bombard the surfaces of the Uranian moons and presumably the planetary rings close to the planet, with total fluences of order 10^{16} cm^{-2} in a period of only 10^4 to 10^5 years. Laboratory studies of the irradiation of methane ice by protons and helium ions with energies of approximately 10 to 2000 keV show that such fluences produce significant darkening and polymerization of the surface (*15*). Similar modification of carbon monoxide ice surfaces is observed, although it proceeds at only a few percent of the rate for methane ice. Darkening of pure water ice is not observed. Particle-produced polymerization can greatly reduce the albedos of exposed surfaces in which carbon-bearing ices are present. Particle modification of Uranian ice surfaces may explain the low albedos of Uranian ring particles and dark areas of the moons, provided that methane and carbon monoxide ices are present in addition to water ice.

Figure 6 shows an overview sketch of the Uranian magnetosphere as revealed by Voyager 2. The magnetosphere is large enough to include at least four of the major satellites nearly all of the time. A nightside aurora is present (*14*), for which particle precipitation may be important, as was predicted (*16*). The most important new aspect of the magnetosphere is the large tilt of the magnetic axis relative to the rotation axis, contrary to predictions made before encounter (*17*).

The Uranian magnetosphere presents a number of unsolved mysteries. One is the electroglow (*14*). Another is the indication that ice sputtering on the Uranian moons may provide a source of water comparable to that found at Saturn if heavy ions are abundant at energies near or above 10 keV

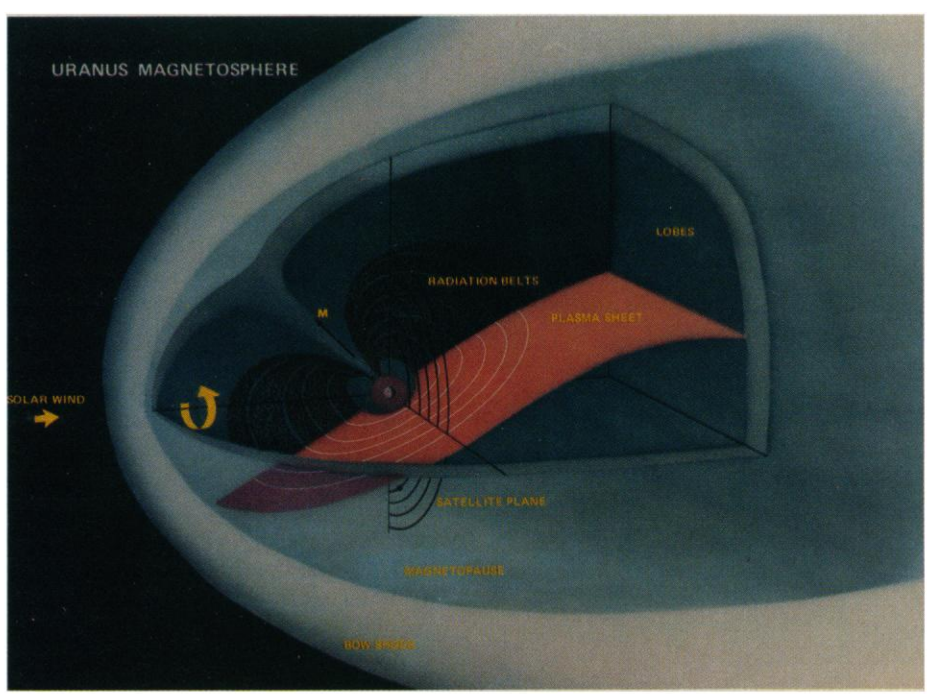

Fig. 6. Overview sketch of the Uranian magnetosphere, showing bow shock and magnetopause, boundary layer, dayside cusp, satellite plane, plasma sheet (shaded), radiation belts, effects of satellite sweeping, and extended hydrogen atmosphere around Uranus. The magnetic and rotation axes are marked.

per nucleus (*16*) even though oxygen ions have not yet been detected by the LECP or the plasma science experiments (*13*). This may mean that oxygen ions are not efficiently accelerated to energies ($\gtrsim$0.6 MeV per nucleon) at which composition data are available or that oxygen ions are preferentially lost.

The Uranian magnetosphere may be characterized by an efficient mechanism for preferentially removing energetic ions, as opposed to electrons, from the radiation belts, even though loss rates due to sweeping by satellites are comparable for ions and electrons at energies observed by the LECP instrument. One candidate mechanism is charge exchange in an extended hydrogen atmosphere if one is present (*14*); another is wave-particle interactions. Preferential ion loss is supported by the observation that the energetic ion β is substantially less than that found at Saturn, whereas the electron β is comparable to Saturnian values. The total plasma β is then much less than 1, so that particle stresses do not greatly distort the field at Uranus. Since large day-night asymmetries are observed in the radiation belts outside the orbit of Umbriel, there may be a significantly nondipolar magnetic field at these distances in which magnetopause currents take an important part.

REFERENCES AND NOTES

1. L. J. Lanzerotti and S. M. Krimigis, *Phys. Today* **38**, 25 (1985).
2. N. F. Ness *et al.*, *Science* **233**, 85 (1986).
3. J. W. Warwick *et al.*, *ibid.*, p. 102.
4. S. M. Krimigis *et al.*, *Space Sci. Rev.* **21**, 329 (1977).
5. S. M. Krimigis *et al.*, *Science* **204**, 998 (1979).
6. Because of damage to the thinnest (2-μm) LECP detector during the Voyager 2 encounter with Saturn's magnetosphere, the lowest energy ion species separated in Uranus' magnetosphere ($\gtrsim$0.6 MeV per nucleon) was higher than that separated during the encounter with Jupiter and Saturn ($\gtrsim$0.2 MeV per nucleon).
7. D. C. Hamilton, D. C. Brown, G. Gloeckler, W. I. Axford, *J. Geophys. Res.* **88**, 8905 (1983).
8. J. F. Carbary and S. M. Krimigis, *Geophys. Res. Lett.* **9**, 1073 (1982).
9. S. M. Krimigis, R. D. Zwickl, D. N. Baker, *J. Geophys. Res.* **90**, 3947 (1985).
10. S. M. Krimigis, in *Proceedings of the Conference on Comparative Study of Magnetospheric Systems* (Centre National d'Etudes Spatiales, Toulouse, France, 1986), pp. 99–124.
11. G. Anagnostopoulos, E. T. Sarris, S. M. Krimigis, *J. Geophys. Res.* **91**, 3020 (1986).
12. S. M. Krimigis *et al.*, *ibid.* **88**, 8871 (1983).
13. H. S. Bridge *et al.*, *Science* **233**, 89 (1986).
14. A. L. Broadfoot *et al.*, *ibid.*, p. 74.
15. A. F. Cheng and L. J. Lanzerotti, *J. Geophys. Res.* **83**, 2597 (1978); L. J. Lanzerotti, W. L. Brown, K. J. Marcantonio, in preparation; L. Calcagno, L. G. Foti, L. Torrisi, G. Strazzullo, *Icarus* **63**, 31 (1985).
16. A. F. Cheng, in *Uranus and Neptune*, J. T. Bergstrahl, Ed. (*NASA Conf. Publ. 2330*, 1984), p. 541; ——— and T. W. Hill, *ibid.*, p. 557.
17. T. W. Hill, *ibid.*, p. 497; G. L. Siscoe, *Icarus* **24**, 311 (1975).

18. We thank the members of the Voyager project and personnel at the Jet Propulsion Laboratory and the Planetary Programs Office, NASA Headquarters, for help and cooperation in carrying out this experiment. We thank J. Carbary, M. Paonessa, B. J. Hook, L. Pacini, J. G. Gunther, D. C. Brown, C. G. Maclennan, and E. V. Bell, II for their enthusiasm and long hours in support of the project. The work of O. Divers (among many others) was essential to the success of our investigation. We thank the Voyager MAG team for making their field model available before publication. Supported by NASA under task I of contract N00024-85-C-5301 and by subcontract at the universities of Kansas and Maryland.

31 March 1986; accepted 5 May 1986

Voyager 2 Radio Observations of Uranus

James W. Warwick, David R. Evans, Joseph H. Romig, Constance B. Sawyer, Michael D. Desch, Michael L. Kaiser, Joseph K. Alexander, Thomas D. Carr, David H. Staelin, Samuel Gulkis, Robert L. Poynter, Monique Aubier, Andre Boischot, Yolande Leblanc, Alain Lecacheux, Bent M. Pedersen, Philippe Zarka

Within distances to Uranus of about 6×10^6 kilometers (inbound) and 35×10^6 kilometers (outbound), the planetary radio astronomy experiment aboard Voyager 2 detected a wide variety of radio emissions. The emission was modulated in a period of 17.24 ± 0.01 hours, which is identified as the rotation period of Uranus' magnetic field. Of the two poles where the axis of the off-center magnetic dipole (measured by the magnetometer experiment aboard Voyager 2) meets the planetary surface, the one closer to dipole center is now located on the nightside of the planet. The radio emission generally had maximum power and bandwidth when this pole was tipped toward the spacecraft. When the spacecraft entered the nightside hemisphere, which contains the stronger surface magnetic pole, the bandwidth increased dramatically and thereafter remained large. Dynamically evolving radio events of various kinds embedded in these emissions suggest a Uranian magnetosphere rich in magnetohydrodynamic phenomena.

Radio emissions from Uranus were first detected through analysis of planetary radio astronomy (PRA) (*1*) data taken during the 5 days before Voyager 2's closest approach to the planet. In Fig. 1, a periodically varying signal is clearly present in the upper 58.8-kHz and upper 78.0-kHz channels as the spacecraft approached Uranus. The planetary signals, which were most intense in the upper channel, increased in amplitude as the spacecraft neared closest approach; strong spacecraft interference can be recognized by its shape as a function of time in both the upper and the lower channels for each frequency. No planetary signals occur at 39.6 kHz except near closest approach and, possibly, at DOY 19.2. This signal appears also at 58.8 kHz and in both upper and lower channels. Many similar, intense signals appear before closest approach at 58.8, 78.0, and 97.2 kHz, but we cannot identify with surety any of these as planetary signals. Emission was relatively weak in the 97.2-kHz channels until the spacecraft was near closest approach. The emission before encounter probably extended continuously from about 40 to 100 kHz.

Opposite states of circular polarization appear in upper and lower channels of the PRA instrument. The relation of upper or lower channel to polarization sense reversed near closest approach, when the direction to the source passed through the plane of the antenna. In the usual definition for radio science, the upper channel at each frequency is polarized in the left-hand sense before and in the right-hand sense after closest approach. Before closest approach, the emission was strongest in the upper channel for each frequency at which emission occurred; after closest approach, the emission was generally strongest in the lower channel for each frequency. With some important exceptions, the emissions were therefore left-hand polarized throughout encounter.

Figure 2 shows overview dynamic spectra covering the 4-day period near closest approach. The great increase and subsequent decrease in intensity is apparent at most frequencies, and there was an enormous extension in emission bandwidth to higher frequencies (up to 800 kHz) that began just before closest approach. This high-frequen-

J. W. Warwick, D. R. Evans, J. H. Romig, C. B. Sawyer, Radiophysics, Inc., Boulder, CO 80301.
M. D. Desch and M. L. Kaiser, Laboratory for Extraterrestrial Physics, Goddard Space Flight Center, Greenbelt, MD 20771.
J. K. Alexander, NASA Headquarters, Washington, DC, 20546.
T. D. Carr, Department of Astronomy, University of Florida, Gainesville, FL 32611.
D. H. Staelin, Research Laboratory of Electronics, Massachusetts Institute of Technology, Cambridge, MA 02319.
S. Gulkis and R. L. Poynter, Jet Propulsion Laboratory, California Institute of Technology, Pasadena, CA 91109.
M. Aubier, A. Boischot, Y. Leblanc, A. Lecacheux, B. M. Pedersen, P. Zarka, Observatoire de Paris, Section d'Astrophysique, 92190 Meudon, France.